

## Radioiodide Imaging and Treatment of ARO Cancer Xenograft in a Mouse Model after Expression of Human Sodium Iodide Symporter

YA-JU HSIEH<sup>1\*</sup>, CHIEN-CHIH KE<sup>4,7\*</sup>, REN-SHYAN LIU<sup>1,2,4,7</sup>, FU-HUI WANG<sup>4,7</sup>,  
KAM-TSUN TANG<sup>5</sup>, CHIN-WEN CHI<sup>3</sup>, FU-DU CHEN<sup>8</sup> and CHEN-HSEN LEE<sup>6</sup>

<sup>1</sup>Institute of Radiological Sciences, <sup>2</sup>Department of Nuclear Medicine, Faculty of Medicine,  
<sup>3</sup>Department and Institute of Pharmacology, School of Medicine, National Yang-Ming University, Taipei;

<sup>4</sup>National PET/Cyclotron Center, <sup>5</sup>Division of Metabolism and Endocrinology,

<sup>6</sup>Division of Transfusion Medicine, Department of Medicine, Taipei Veterans General Hospital, Taipei;

<sup>7</sup>Molecular and Genetic Imaging Core, NRPGM, Taipei;

<sup>8</sup>Institute of Radiological Sciences, Central Taiwan University of Science and Technology, Taichung, Taiwan, R.O.C.

**Abstract.** Background: Most undifferentiated and anaplastic thyroid carcinomas are not sensitive to <sup>131</sup>I therapy due to their lost ability for iodide accumulation. This study aims to restore the iodide uptake by transferring and expressing human sodium iodide symporter (hNIS) in these cancer cells for <sup>131</sup>I gene therapy. Materials and Methods: hNIS cDNA expression vector was transfected into wild-type anaplastic thyroid cancer cells (ARO-W) which do not concentrate iodide. Stable transfected cells were isolated (ARO-S) and analyzed by RT-PCR, radioiodide uptake and immunocyto-chemistry staining. <sup>131</sup>I imaging and treatment were performed on mice bearing ARO-W and ARO-S xenograft tumors and tumor volume was recorded. Results: The ARO-S cells showed clear hNIS expression on the cell membrane and accumulated 87-fold and 4.4-fold radioiodide of that of wild-type cells in vitro and in vivo, respectively. Radioiodide uptake was dependent on cell number and reached a maximum level at 20 minutes in vitro. The half life of radioiodide efflux was 12 minutes and 12 hours in vitro and in vivo, respectively. Administration of a

therapeutic dose of <sup>131</sup>I into mice bearing ARO-S tumors effectively inhibited tumor growth as compared to control mice. Conclusion: Our results suggest the potential of hNIS-mediated <sup>131</sup>I gene therapy on anaplastic thyroid cancer cells.

Thyroid cancer, accounting for about 1% of all human cancers, is the most frequent malignancy of the endocrine system. It is generally a treatable disease with good prognosis following the current treatment protocol, however this does not include 30% of the cases, which are classified as dedifferentiated (1). To date, radioiodide remains the major diagnostic and therapeutic tool for treatment of differentiated thyroid carcinomas because most retain a certain degree of iodide concentrating capacity. However, this is not true for anaplastic thyroid cancer because it usually does not concentrate iodide (2). Anaplastic thyroid carcinoma represents less than 2% of all thyroid cancers and is an aggressive form of thyroid cancer (3). With aggressive multimodality treatment, patients with anaplastic thyroid carcinoma have improved local disease control but the survival rate remains low (4).

In recent years, cloning of rat and human sodium iodide symporter (NIS) has not only opened a gate for better understanding the mechanism by which some thyroid cancers lose or have a reduced ability for iodide uptake, but also, most importantly, has offered a new strategy for restoring the therapeutic effect of radioiodide in cancers which have impaired iodide concentrating capacity (5). The human sodium iodide symporter (hNIS) gene was first cloned in 1996 and was found located on chromosome 19p12-13.2 with an open reading frame of 1,929 nucleotides. The nucleotide sequence consists of 15 exons interrupted by 14 introns and encodes a glycoprotein of 643 amino acids.

\*Both authors contributed equally to this work.

**Abbreviations:** SCID, severe combined immune defects; NIS, sodium iodide symporter.

**Correspondence to:** Ren-Shyan Liu, MD, National PET and Cyclotron Center, Taipei Veterans General Hospital, No. 201, Sec. 2, Shih-Pai Road, Taipei 112, Taiwan, R.O.C. Fax: +886 2 28749431, e-mail: rslu@vghtpe.gov.tw

**Key Words:** Radioiodide imaging, mouse model, xenograft, SCID, severe combined immune deficiency, sodium iodide symporter, anaplastic thyroid cancer, ARO cells.

hNIS is a membrane protein with proposed to have 13 putative transmembrane domains, an extracellular amino-terminus and an intracellular carboxyl-terminus with 3 putative *N*-linked glycosylation sites at positions 225, 485 and 497. It is expressed at the basolateral membrane of thyroid follicular cells and accounts for the transportation of one  $\Gamma^-$  ion and two  $\text{Na}^+$  ions into cell (5-10).

Several investigators have investigated the feasibility of expressing NIS in a variety of cancer types, including melanoma, cervical (11), breast (11, 12), glioma (13), hepatoma (14), prostate (15-17), non-small cell lung (18), myeloma (19), ovarian (20) and pancreatic (21). Transfection of cell lines of these cancer types with NIS cDNA enabled them to concentrate iodide. A distinct iodide concentration was seen *via in vitro* radioiodide uptake or *in vivo* imaging of xenografts derived from these NIS-transduced cell lines. The results showed promise in the field of NIS gene therapy. Several investigators have reported  $^{131}\text{I}$  therapy on NIS-transduced tumors. A remarkable reduction in tumor volume or an inhibition in tumor growth was observed (12, 17, 20, 22).

The same algorithm has also been applied to thyroid related cancers. Undifferentiated thyroid cancer cells of rats stably transfected with rat NIS showed effective accumulation of radioiodide (23). Lee *et al.* (24) also demonstrated that transfection of rat NIS into anaplastic thyroid cancer (ARO) cells successfully triggered the uptake of radioiodide,  $^{99\text{m}}\text{Tc}$  and  $^{188}\text{Re}$  *in vivo* as well as *in vitro*. These results show the great potential of imaging and therapy in rat NIS gene delivered into anaplastic thyroid carcinoma. To further assess the feasibility of human NIS in anaplastic thyroid cancer gene therapy, we determined whether human sodium iodide symporter could be stably transfected into anaplastic thyroid cancer cell line ARO. *In vitro* hNIS gene expression, radioiodide uptake and efflux were determined, while *in vivo* uptake of radioiodide was assessed using a  $\gamma$ -camera. The growth of tumors treated with  $^{131}\text{I}$  was finally examined to evaluate the possibility of hNIS gene therapy in anaplastic thyroid cancer.

## Materials and Methods

**Construction of a hNIS-expressing vector.** The hNIS cDNA cloned in pcDNA3 as a clone designated FL\*-hNIS/pcDNA3 was kindly provided by Dr. Sissy Jhiang (Ohio state University). The full length hNIS cDNA was digested with BamHI and XhoI from FL\*-hNIS/pcDNA3 and cloned into the BglII and SalI digested pIRES2-EGFP vector (BD Bioscience Clontech, USA). The hNIS in pIRES2-EGFP vector was under the control of cytomegalovirus promoter and designated as hNIS/pIRES2-EGFP.

**Cell culture and stable cell line generation.** ARO-W cells were cultured in RPMI-1640 medium (Invitrogen, Carlsbad, USA) supplemented with 10% fetal bovine serum, 2 mM L-glutamine,

100 U/ml penicillin and 100  $\mu\text{g}/\text{ml}$  streptomycin. Forty-eight hours after hNIS/pIRES2-EGFP transfection into cells using jetPEI (Q-Biogene, Illkirch, France) with 10 N/P ratio according to the manufacturer's instructions, cells were subcultured and maintained in 1500  $\mu\text{g}/\text{ml}$  G418 (Sigma, St. Louis, USA) selection medium. After approximately 2 weeks, the single, well-surviving cell clones were isolated and subjected to testing for hNIS expression.

**hNIS gene expression measurement using RT-PCR.** ARO-W cells and ARO hNIS cell stable clones were cultured in 60 mm dishes. After cells reached confluency, they were trypsinized and total RNA was isolated using the RNeasy mini kit (Qiagen Sciences, Maryland, USA). First strand cDNA was synthesized with 2  $\mu\text{g}$  total RNA using ReverAid reverse transcription kit (Fermentas, Burlington, Canada). hNIS cDNA was verified by polymerase chain reaction in 50  $\mu\text{l}$  of reaction volume with forward primer 5'-TCAGCACAGCATCCACCAG-3' and reverse primer 5'-GGGCACCGTAATAGAGATAG-3'. Briefly, samples were denatured at 95°C for 4 min and subjected to 30 cycles at 95°C, 52°C and 72°C for 30 sec each and final extension at 72°C for 5 min. PCR products were electrophoresed on a 2% agarose gel and amplified bands were detected by ethidium bromide staining.

**In vitro radioactive iodide uptake and efflux.** Cellular uptake of iodide was measured *in vitro* as described by Weiss *et al.* (25) and Shin *et al.* (26) with slight modification. To select a cell clone that possesses the best ability for iodide uptake within several clones, ARO hNIS stable cell clones and ARO-W were inoculated into 12-well plates at the same rate ( $5 \times 10^5$ ). After a 24-h incubation, cells were incubated with 1  $\mu\text{Ci}$  of  $^{131}\text{I}$  in 0.5 ml Hanks' balanced salt solution (HBSS) containing 10  $\mu\text{M}$  NaI at 37°C for 1 hour. Cells were then washed as quickly as possible with 1 ml iodide-free ice-cold HBSS buffer, detached with trypsin and resuspended in 1 ml HBSS. The radioactivity was measured using Cobra II autogamma counter (Packard Instrument, CT, USA). The clone with the highest radioiodide uptake was selected and designated as ARO-S. The relationship between radioiodide uptake and cell number was then assessed on ARO-S cells. Briefly, a dilution series of ARO-S and ARO-W cells were inoculated into 12-well plates over a range of  $3 \times 10^4$  to  $5 \times 10^5$  cells per plate. After 24 hours, cells were incubated with 0.5 ml HBSS containing 10  $\mu\text{M}$  NaI and 0.1  $\mu\text{Ci}$   $^{125}\text{I}$  at 37°C for 1 hour. Cells were collected and  $\gamma$ -counted as above. The time course of  $^{125}\text{I}$  uptake by ARO-S was determined by inoculating cells into 12-well plates. After 24 hours, cells were washed with HBSS buffer and then incubated with 0.1  $\mu\text{Ci}$  of  $^{125}\text{I}$  in pre-warmed HBSS containing 10  $\mu\text{M}$  NaI for 3, 6, 10, 15, 20, 25, 30, 35, 45, 55 or 65 minutes. Cells were then rapidly washed with HBSS and trypsinized and resuspended in 1 ml HBSS. The radioactivity was measured using a  $\gamma$ -counter.

To determine the  $^{125}\text{I}$  efflux, ARO-S cells were incubated for 1 hour with 0.1  $\mu\text{Ci}$  of  $^{125}\text{I}$  in pre-warmed HBSS containing 10  $\mu\text{M}$  NaI. After the cells had been washed twice, fresh non-radioactive HBSS was added. The cells were again incubated for 3, 6, 9, 12, 15, 20, 30, 40, 50, 60, 120 or 180 min and immediately collected and  $\gamma$ -counted, as described above.

**Immunocytochemistry study.** ARO-S cells were grown on 22 mm x 22 mm coverslips (Marienfeld, Lauda-Königshofen, Germany). After a 24-h incubation, cells were rinsed with phosphate buffered-

saline (PBS) for 3 times and then fixed in 4% paraformaldehyde for 15 min at room temperature. After three 5-min washes in PBS, the cells were permeabilized with 0.1% Triton X-100 in PBS/CM/BSA (PBS with 0.1 mM CaCl<sub>2</sub>, 1mM MgCl<sub>2</sub> and 0.2% BSA) for 10 min. After three 5-min washes in PBS, the cells were incubated with a 1:100 dilution of mouse anti-hNIS polyclonal antibody (Chemicon, Temecula, USA) for 1 hour at room temperature and rewashed in PBS. They were then incubated with a 1:200 dilution of tetramethylrhodamine isothiocyanate-conjugated goat anti-mouse IgG (Santa Cruz Biotechnology, Santa Cruz, USA) for 1 hour at room temperature, washed in PBS and incubated in Bisbenzimidazole H33342 for 30 minutes at room temperature. After three final PBS washes (5 min each), the cells were mounted with mounting solution. Fluorescent images of cells were observed using a Leica TCS SP5 confocal microscope.

**In vivo imaging of hNIS-expressing tumor-bearing mice.** To evaluate radioiodide uptake *in vivo*, 5x10<sup>6</sup> ARO cells and 7x10<sup>6</sup> ARO-S cells were inoculated subcutaneously into left and right flanks of the thorax region of severe combined immune defects (SCID) mice. After tumors had grown for 1-2 weeks and the tumor volume had reached about 10 mm in diameter, scintigraphic imaging was performed 1, 3, 5, 7, 14, 28 and 48 hours after 50  $\mu$ Ci <sup>131</sup>I injection through the tail vein. Mice were anesthetized using isoflurane according to general gaseous anesthesia (40% O<sub>2</sub> / 60% N<sub>2</sub>O / 1% halothane) and placed prone at a distance of 6 cm under a 4-mm pinhole collimator equipped on the Siemens dual-head gamma camera (E CAM, Siemens, Hoffman Estates, USA). Each image at each time point was taken for 20 minutes. Region of interests (ROIs) on both ARO-W and ARO-S tumors in each image were analyzed.

**In vivo <sup>131</sup>I therapy.** The ARO-S tumor model was established as above to assess the effect of <sup>131</sup>I therapy on the hNIS-expressing anaplastic thyroid cancer cells. Two weeks after cell inoculation, nine mice bearing ARO-S tumor xenografts (~1 cm in diameter) were intraperitoneally injected with 1.5 mCi <sup>131</sup>I; the same volume of normal saline was administered to six mice as a control group. The tumor size was measured twice a week after the start of treatment and the tumor volume was calculated using the equation: VT (mm<sup>3</sup>) = L x W x D x 0.52 where VT is the estimated tumor volume, and L, W and D are the length (mm), width (mm) and depth (mm) of the tumor, respectively. All mice were monitored for 9 weeks.

## Results

**hNIS gene expression using RT-PCR.** Figure 1 shows 1% agarose gel electrophoresis of ethidium bromide-stained PCR products amplified by hNIS forward and reverse primers after reverse-transcription of total RNA. A total of 547 base pair bands were observed in lane 1~4 which represent 4 stable clones. Lane 6 is the positive control (hNIS-bearing plasmid as PCR template); ARO-W cells (lane 5) and negative control (template-free PCR, lane 7) showed no specific bands.

**Radioiodide uptake of stable clones and the correlation between radioactivity and cell number.** Figure 2A shows the

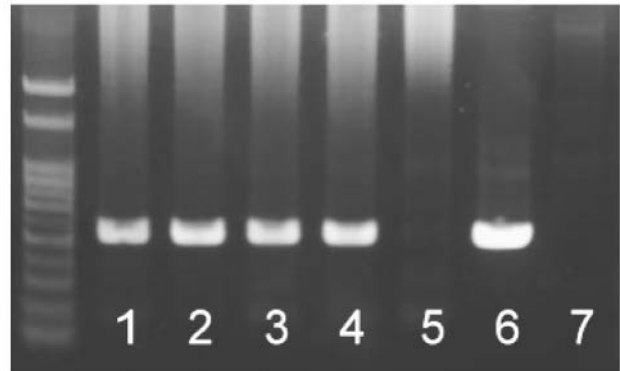


Figure 1. Electrophoresis result of 4 picked-up ARO stable clones and wild-type cells. Lane 1~4 represent ethidium bromide-stained 4 stable clones and show clearly expressing hNIS while lane 5 shows that for ARO-W cells which expressed no hNIS. Lane 6 and 7 are positive and negative control, respectively.

result of radioiodide uptake of 4 stable clones and 2 mixed clones (transfected cells without isolation). When treated with 1  $\mu$ Ci <sup>131</sup>I for 1 hr, the 4 stable clones showed higher radioiodide uptake than did the ARO-W cells or the 2 mixed clones. Furthermore, ARO-S (stable clone No. 2) was assayed using <sup>125</sup>I for the uptake assay and the results showed a high correlation ( $r^2=0.9985$ ) between cell number and radioiodide uptake (Figure 2B). ARO-S was thus used in the subsequent experiments in this study.

**Kinetics of radioiodide uptake in vitro.** Accumulation of <sup>125</sup>I in ARO-S cells reached a maximum level at 20 minutes and half-maximal level within 6 minutes. The <sup>125</sup>I uptake of ARO-S was 87-fold higher than that of ARO-W cells. Transportation of iodide into the hNIS transfectant cells was rapidly initiated as soon as cells were exposed to the iodide. The uptake of iodide was time-dependent at the initial incubation till iodide accumulation reached the plateau (Figure 3).

**Radioiodide efflux assay.** Radioiodide was rapidly lost from cells (Figure 4). The  $t_{1/2}$  of the iodide efflux of ARO-S cells was 12 min and 80% efflux was reached after 50 min. Namely, iodide could be transported into hNIS-stably transfected ARO-S cells but was not trapped in the cells.

**Immunocytochemistry study.** Immunocytochemistry analysis revealed that the hNIS proteins were expressed on the plasma membrane of ARO-S cells (Figure 5). With stable transfection with hNIS/pIRES2-EGFP, green fluorescence was also observed in ARO-S cells. The composite image of hNIS (red), EGFP (green) and nuclei (blue) strongly revealed the localization of hNIS in the cells.

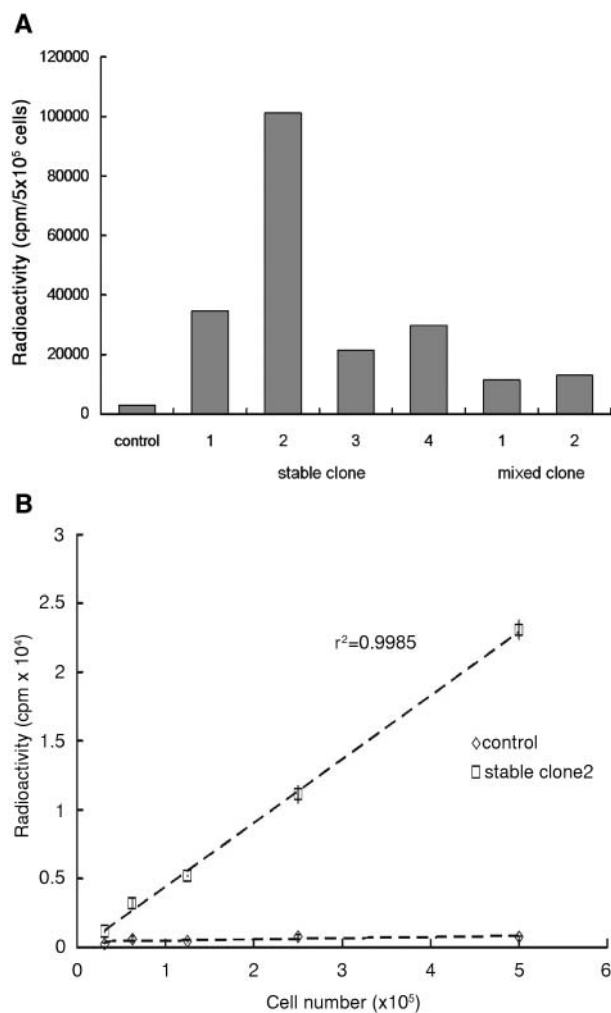


Figure 2. *In vitro* radioiodide uptake assay of ARO cells versus cell number. Different numbers of ARO-W cells (◇) coupled with ARO transduced clones (stable clones and mixed clones) were inoculated and underwent <sup>131</sup>I uptake assay. Each clone showed a correlation between radioiodide uptake and cell number; a remarkably high uptake was seen in ARO-S (stable clone 2) (A). Radioiodide uptake assay using <sup>125</sup>I was further performed on ARO-S (□) with triplicated tests at each data point. The linear regression analysis showed a high correlation between cell number and radioiodide uptake in <sup>125</sup>I uptake assays and regression coefficient was  $r^2=0.9986$ , respectively (B). All values are mean and standard deviation ( $n=3$ ).

*In vivo* imaging of hNIS-expressing tumor-bearing mice. Images of tumor-bearing mice acquired at various time points showed higher <sup>131</sup>I accumulation in hNIS-expressing ARO-S tumors than ARO-W tumors, which only showed a background uptake level (Figure 6). Radioactivity of both tumors and thyroid were obtained by selection of regions of interests (ROIs) on the corresponding regions (Figure 7). Both ARO-S and ARO-W tumors reached the highest

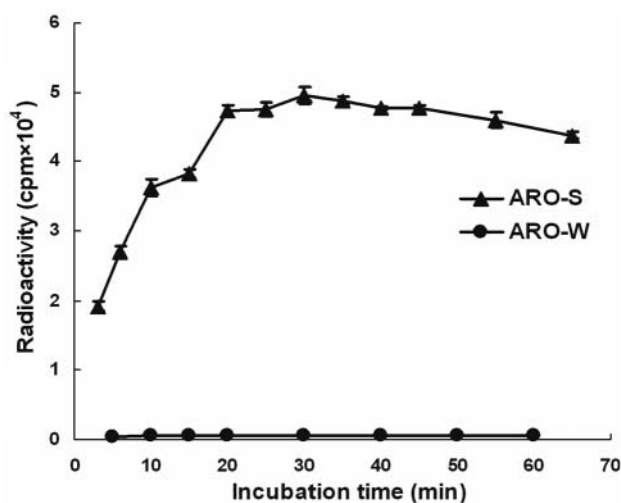


Figure 3. Time-activity curve of <sup>125</sup>I uptake in ARO-S cells. Uptake was initiated by incubating ARO-S and ARO-W cells with the same number of cells with 0.1  $\mu$ Ci <sup>125</sup>I in 0.5ml HBSS. After incubation for 3, 6, 10, 15, 20, 25, 30, 35, 45, 55 and 65 minutes, cells were washed, collected and the radioactivity was counted. Values are mean and standard deviation of triplicate wells.

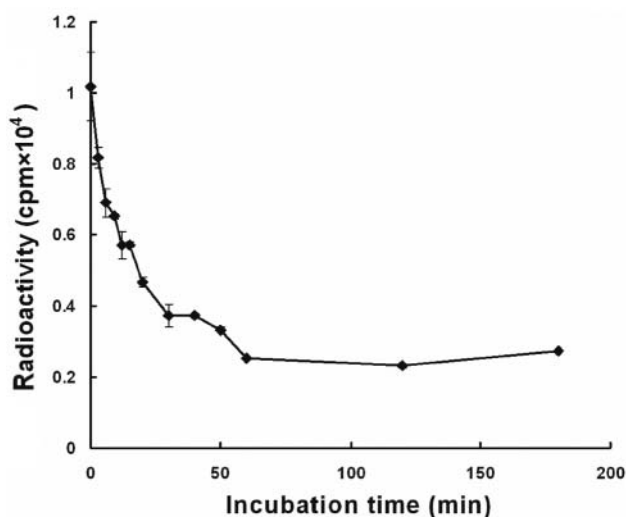


Figure 4. Iodide efflux from ARO-S cells after 1-h incubation with <sup>125</sup>I. At various time points, the cell radioactivity was determined after removal of the buffer. Radioiodide was cleared rapidly: 50% and 80% radioiodide efflux occurred at 12 and 50 minutes. Values are mean and standard deviation of the counts per minute (cpm) of triplicate wells.

radioiodide uptake value less than 1 hour after *i.p.* injection of <sup>131</sup>I and then cleared rapidly. ARO-S tumors accumulated 4.4-fold radioiodide of that of wild-type tumors. The thyroid accumulated iodide slowly at first, reaching a plateau about 14 hours later, and then maintained this level for several hours followed by clearance.

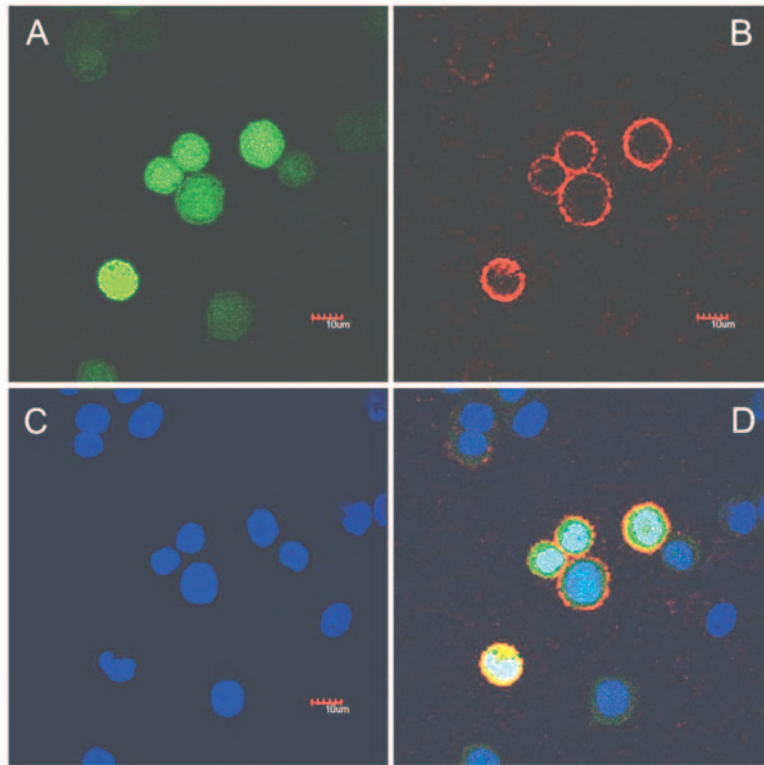


Figure 5. Immunofluorescent staining of hNIS in ARO-S cells. EGFP expression (A, green) was observed throughout cells while hNIS expression was detected on the cell membrane by immunostaining with hNIS primary antibody/TRITC-conjugated 2nd antibody (B, red). The cell nuclei was shown by H33334 dye specific binding to nucleic acid (C, blue). The composite image (D) explicitly demonstrates the localization of hNIS which was expected to be expressed on the cell membrane.

**Radioiodide therapy in vivo.** ARO-S tumors treated with  $^{131}\text{I}$  showed significant growth inhibition while ARO-S tumors treated with saline increased rapidly in size with time (Figure 8).

## Discussion

This study describes the success of introducing the human sodium iodide symporter gene into anaplastic thyroid cancer cells, followed by restoration of iodide-concentrating ability. The hNIS gene expression of ARO stable cells was confirmed by *in vitro* radioiodide uptake, efflux, RT-PCR, immunocytochemistry and *in vivo* radioiodide imaging, as well as radioiodide therapy. Although transfer of NIS into anaplastic thyroid cancer cells had been reported previously (24), the effect of radioiodide therapy on this model has never been reported.

In this study we constructed a dual reporter vector which mediates the expression of hNIS and enhanced green fluorescent protein (EGFP). Such a vector provides two different imaging readouts of gene expression. EGFP provides an effective fluorescent readout and is widely used in cell-based fluorescence imaging while hNIS serves as a

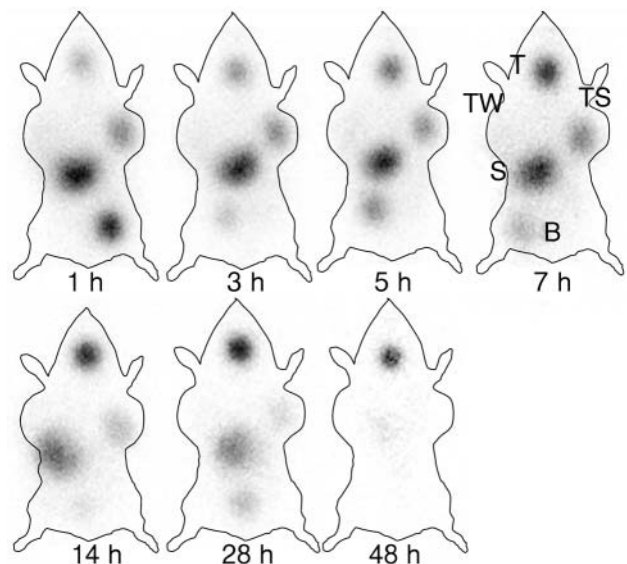


Figure 6. *In vivo*  $^{131}\text{I}$  scintigraphic imaging on SCID mice bearing hNIS-expressing and non-expressing ARO tumors. Sequential images obtained at 1, 3, 5, 7, 14, 28 and 48 hours showed obvious accumulation of iodide in the thyroid, stomach, bladder, and tumor expressing hNIS. The accumulation of iodide was not clearly visualized on ARO-W tumors. T, thyroid; TS, ARO-S tumor; TW, ARO wild-type tumor; S, stomach; B, bladder.

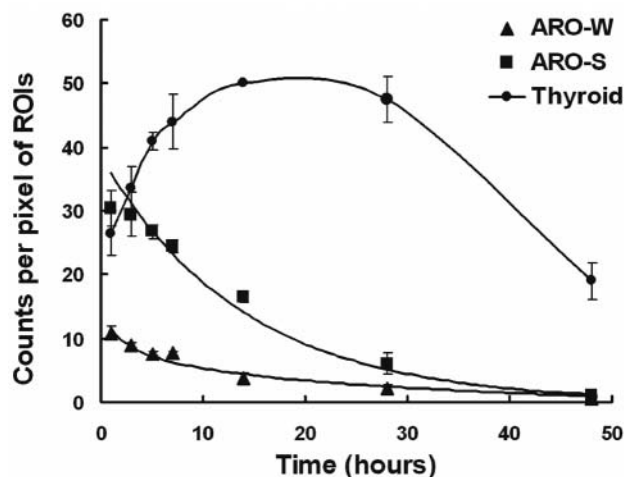


Figure 7. *In vivo* radioiodide uptake and efflux of ARO tumors. ARO-S tumors rapidly accumulated  $^{131}\text{I}$  after injection while ARO-W tumors showed no significant uptake of iodide.  $T_{1/2}$  of  $^{131}\text{I}$  in ARO-S tumor was approximately 12 hours; 20% of  $^{131}\text{I}$  was retained in ARO-S tumors at 28 hours after administration. At 48 hours, the uptake of  $^{131}\text{I}$  was similar in ARO-S and ARO-W tumors.

promising therapeutic and nuclear imaging probe. Both reporter genes are under the control of the same CMV promoter and transcribe into a bicistronic mRNA by means of internal ribosomal entry site (IRES) which enables coexpression of both genes but separate translation (27). In this system, EGFP serves as a useful indicator for monitoring gene delivery and expression, and provides an easy way for stable clone screening in our study. Furthermore, with coexpression of two reporter genes, we can monitor hNIS expression *via* confirming the EGFP expression by fluorescence microscopy.

Shin *et al.* showed that the radioiodide uptake, luciferase assay, and scintigraphic and luminescence imaging of SK-HEP1 cells stably transfected with IRES-linked NIS and luciferase genes, correlated well with viable cell numbers (26). Our current study also showed that the uptake of iodide in hNIS-expressing ARO cells was related to the cell number. This result indicates that the viable cell number can be estimated by radioiodide uptake using hNIS gene expression.

We examined the kinetics of radioiodide accumulated in ARO-S and ARO-W tumors on the same mice. In the ARO-S tumors, uptake of  $^{131}\text{I}$  reached 50% at 12 hour post administration and fell to the background level after 48 hours. Without any further trapping mechanism, there is only the transient uptake of radioiodide in ARO-S tumors. Lack of iodide organification in the cell is the major obstacle in our model of radioiodide gene therapy.

In the  $^{131}\text{I}$  treatment experiment, the volume of ARO-S tumors decreased 30% within 3 weeks after  $^{131}\text{I}$  administra-

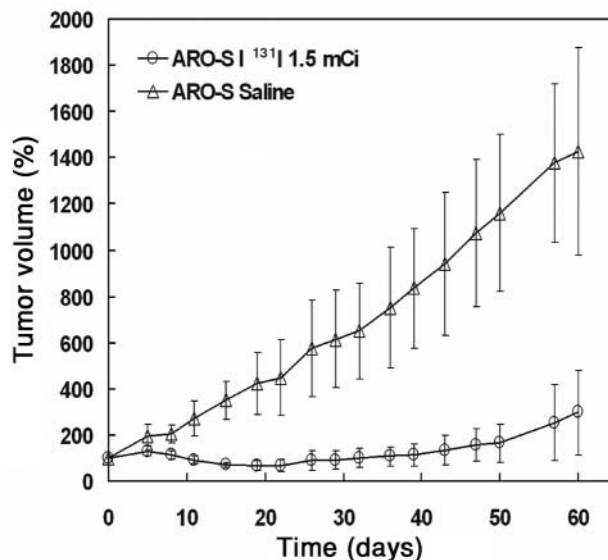


Figure 8. *In vivo*  $^{131}\text{I}$  therapy of ARO-S tumors. Nine mice bearing ARO-S xenografts were intraperitoneally injected  $^{131}\text{I}$  and six ARO-S xenograft-bearing mice were treated with saline as control. Tumor growth was recorded twice a week. The group treated with  $^{131}\text{I}$  showed inhibition of tumor growth while tumors in control group grew rapidly within 9 weeks.

tion. Effective inhibition of tumor growth was observed as compared to the control group. A 3 mCi of  $^{131}\text{I}$  therapy dose had previously been tried in our model according to the literature (12, 20). However, mice suffered severe diarrhea and died 2 weeks after administration of 3 mCi  $^{131}\text{I}$ . Intestinal edema was found. This result is reasonable because in mice, a high level of radioiodide was found accumulated in the gastrointestinal tissue (Figure 6), due to a high expression of gastric NIS in rodents (28). The death of mice may have been caused by choosing SCID mice as our animal model. SCID mice are known to have several immune defects and increased susceptibility to radiation damage (29). Dingli *et al.* reported  $^{131}\text{I}$  therapy of NIS-transfected myeloma in SCID mice (19). The therapeutic dose was calculated to be 1 mCi based on the biodistribution result. This dose completely eradicated the myeloma tumor xenografts they used. However, the inherent high radiosensitivity of myeloma may contribute to the therapy effect. Thus we adopted 1.5 mCi as therapeutic dose and the tumor growth was effectively inhibited during the 9-week observation.

The problem of rapid efflux of radioiodide from cells or tumors was encountered in our study. The *in vitro* study showed a 12 minute  $t_{1/2}$  of  $^{125}\text{I}$  efflux, while a 12 hour  $t_{1/2}$  of  $^{131}\text{I}$  efflux was found in the *in vivo* study. Human NIS and thyroid peroxidase (TPO) genes were coexpressed in non-small cell lung cancer (NSCLC) cell lines by Huang *et al.* (18) and increased iodide uptake and retention was observed

as compared to NIS gene transfection only. This approach offers an effective way to overcome this disadvantage in NIS gene therapy. Since efflux is rapid from tumors, fractionated doses of  $^{131}\text{I}$  could be considered as another approach. The actual effect remains to be confirmed.

## Conclusion

A hNIS gene-mediated radioiodide therapy in anaplastic thyroid cancer has been demonstrated. hNIS-transfected ARO cells were shown to transiently accumulate iodide both *in vitro* and *in vivo*. The growth of tumors was apparently suppressed after treatment with  $^{131}\text{I}$ . Such a result indicates the feasibility and potential of NIS gene therapy in anaplastic thyroid cancer. Further investigations, such as viral-transfer of NIS and tissue-specific expression are ongoing in our laboratory.

## Acknowledgements

This work was supported by grant VGH94-363-2 and V95D-002 from Taipei Veteran General Hospital (2005-2006), Taipei, Taiwan, R.O.C.

## References

- Schmutzler C and Koehrl J: Innovative strategies for the treatment of thyroid cancer. *Eur J Endocrinol* 143: 15-24, 2000.
- Beierwaltes WH: The treatment of thyroid carcinoma with radioactive iodine. *Semin Nucl Med* 8: 79-94, 1979.
- Pasieka, JL: Anaplastic thyroid cancer. *Current opinion in oncology* 15: 78-83, 2003.
- Giuffrida D and Gharib H: Anaplastic thyroid carcinoma: Current diagnosis and treatment. *Ann Oncol* 11: 1083-1089, 2000.
- Dai G, Levy O and Carrasco N: Cloning and characterization of the thyroid iodide transporter. *Nature* 379: 458-460, 1996.
- Smanik PA, Liu Q, Furminger TL, Ryu K, Xing S, Mazzaferri EL and Jhiang SM: Cloning of the human sodium iodide symporter. *Biochem Biophys Res Commun* 226: 339-345, 1996.
- Smanik PA, Ryu KY, Theil KS, Mazzaferri EL and Jhiang SM: Expression, exon-intron organization, and chromosome mapping of the human sodium iodide symporter. *Endocrinol* 138: 3555-3558, 1997.
- Levy O, De la Vieja A and Carrasco N: The  $\text{Na}^+/\text{I}^-$  symporter (NIS): Recent advances. *J Bioenerg Biomembr* 30: 195-206, 1998.
- Dohan O and Carrasco N: Advances in  $\text{Na}^+/\text{I}^-$  symporter (NIS) research in the thyroid and beyond. *Mol Cell Endocrinol* 213: 59-70, 2003.
- Eskandari S, Loo D, Dai G, Levy O, Wright EM and Carrasco N: Thyroid  $\text{Na}^+/\text{I}^-$  symporter. Mechanism, stoichiometry, and specificity. *J Biol Chem* 272: 27230-27238, 1997.
- Boland A, Ricard M, Opolon P, Bidart JM, Yeh P, Filetti S, Schlumberger M and Perricaudet M: Adenovirus-mediated transfer of the thyroid sodium/iodide symporter gene into tumors for a targeted radiotherapy. *Cancer Res* 60: 3484-3492, 2000.
- Dwyer RM, Bergert ER, O'Connor MK, Gendler SJ and Morris JC: *In vivo* radioiodide imaging and treatment of breast cancer xenografts after MUC1-driven expression of the sodium iodide symporter. *Clin Cancer Res* 11: 1483-1489, 2005.
- Cho JY, Xing S, Liu X, Buckwalter TL, Hwa L, Sferra TJ, Chiu IM and Jhiang SM: Expression and activity of human  $\text{Na}^+/\text{I}^-$  symporter in human glioma cells by adenovirus-mediated gene delivery. *Gene Ther* 7: 740-749, 2000.
- Sieger S, Jiang S, Schonsiegel F, Eskerski H, Kubler W, Altmann A and Haberkorn U: Tumour-specific activation of the sodium/iodide symporter gene under control of the glucose transporter gene 1 promoter (GTI-1.3). *Eur J Nucl Med Mol Imaging* 30: 748-756, 2003.
- Haberkorn U, Kinscherf R, Kissel M, Kubler W, Mahmut M, Sieger S, Eisenhut M, Peschke P and Altmann A: Enhanced iodide transport after transfer of the human sodium iodide symporter gene is associated with lack of retention and low absorbed dose. *Gene Ther* 10: 774-780, 2003.
- Dwyer RM, Schatz SM, Bergert ER, Myers RM, Harvey ME, Classic KL, Blanco MC, Frisk CS, Marler RJ, Davis BJ, O'Connor MK, Russell SJ and Morris JC: A preclinical large animal model of adenovirus-mediated expression of the sodium-iodide symporter for radioiodide imaging and therapy of locally recurrent prostate cancer. *Mol Ther* 12: 835-841, 2005.
- Spitzweg C, O'Connor MK, Bergert ER, Tindall DJ, Young CY and Morris JC: Treatment of prostate cancer by radioiodine therapy after tissue-specific expression of the sodium iodide symporter. *Cancer Res* 60: 6526-6530, 2000.
- Huang M, Batra RK, Kogai T, Lin YQ, Hershman JM, Lichtenstein A, Sharma S, Zhu LX, Brent GA and Dubinett SM: Ectopic expression of the thyroperoxidase gene augments radioiodide uptake and retention mediated by the sodium iodide symporter in non-small cell lung cancer. *Cancer Gene Ther* 8: 612-618, 2001.
- Dingli D, Diaz RM, Bergert ER, O'Connor MK, Morris JC and Russell SJ: Genetically targeted radiotherapy for multiple myeloma. *Blood* 102: 489-496, 2003.
- Dwyer RM, Bergert ER, O'Connor MK, Gendler SJ and Morris JC: Sodium iodide symporter-mediated radioiodide imaging and therapy of ovarian tumor xenografts in mice. *Gene Ther* 13: 60-66, 2006.
- Dwyer RM, Bergert ER, O'Connor MK, Gendler SJ and Morris JC: Adenovirus-mediated and targeted expression of the sodium/iodide symporter permits *in vivo* radioiodide imaging and therapy of pancreatic tumors. *Hum Gene Ther* 17: 661-668, 2006.
- hen L, Altmann A, Mier W, Eskerski H, Leotta K, Guo L, Zhu R and Haberkorn U: Radioiodine therapy of hepatoma using targeted transfer of the human sodium/iodide symporter gene. *J Nucl Med* 47(5): 854-862, 2006.
- Shimura H, Haraguchi K, Miyazaki A, Endo T and Onaya T: Iodide uptake and experimental  $^{131}\text{I}$  therapy in transplanted undifferentiated thyroid cancer cells expressing the  $\text{Na}^+/\text{I}^-$  symporter gene. *Endocrinol* 138: 4493-4496, 1997.
- Lee YJ, Chung JK, Shin JH, Kang JH, Jeong JM, Lee DS and Lee MC: *In vitro* and *in vivo* properties of a human anaplastic thyroid carcinoma cell line transfected with the sodium iodide symporter gene. *Thyroid* 14: 889-895, 2004.
- Weiss SJ, Philip NJ and Grollmann EF: Iodine transport in a continuous line of cultured cells from rat thyroid. *Endocrinology* 114: 1090-1098, 1984.

- 26 Shin JH, Chung JK, Kang JH, Lee YJ, Kim KI, So Y, Jeong JM, Lee DS and Lee MC: Noninvasive imaging for monitoring of viable cancer cells using a dual-imaging reporter gene. *J Nucl Med* 45: 2109-2115, 2004.
- 27 Jackson RJ and Kaminski A: Internal initiation of translation in eukaryotes: the picornavirus paradigm and beyond. *RNA* 1: 985-1000, 1995.
- 28 Kotani T, Ogata Y, Yamamoto I, Aratake Y, Kawano JI, Suganuma T and Ohtaki S: Characterization of gastric Na<sup>+</sup>/I<sup>-</sup> symporter of the rat. *Clin Immunol Immunopath* 89: 271-278, 1998.
- 29 Shultz LD, Lang PA, Christianson SW, Gott B, Lyons B, Umeda S, Leiter E, Hesselton R, Wagar EJ, Leif JH, Kollet O, Lapidot T and Greiner DL: NOD/LtSz-Rag1<sup>null</sup> mice: an immunodeficient and radioresistant model for engraftment of human hematolymphoid cells, HIV infection, and adoptive transfer of NOD mouse diabetogenic T cells. *J Immunol* 164: 2496-2507, 2000.

*Received March 2, 2007*

*Revised May 25, 2007*

*Accepted May 30, 2007*